Residual Stress Impingement Methods and Environmental Fracture Susceptibility

Subjects: Metallurgy & Metallurgical Engineering
Contributor: Matthew McMahon

Metallic components undergo stress due to externally applied forces and/or internal residual forces, with the latter often originating from thermally induced deformation during production or from the forming and machining processes. Over time in service, these stresses may act in concert with the surrounding environment, component geometry, surface defects, corrosion, and more to induce subcritical damage in the form of fatigue, corrosion fatigue, or environmentally assisted cracking (EAC). To combat such degradation, numerous residual stress impingement (RSI) methods have been developed with varying levels of efficacy and ease of use. This entry summarizes the benefits and detriments of leading RSI treatments towards corrosion, corrosion fatigue, and EAC in a range of engineering alloys as a function of material hardness.

Keywords: residual stress ; stress corrosion ; corrosion fatigue ; laser peening ; low plasticity burnishing ; shot peening

1. Introduction

Metallic components undergo stress due to externally applied forces and/or internal residual forces, with the latter often originating from thermally induced deformation during production or from the forming and machining processes. Over time in service, these stresses may act in concert with the surrounding environment, component geometry, surface defects, corrosion, and more to induce subcritical damage in the form of fatigue, corrosion fatigue, or environmentally assisted cracking (EAC). These phenomena affect the majority of alloys under the right conditions, and all require a minimum stress intensity (K)/stress intensity amplitude (ΔK) condition to initiate and propagate [1]. The ubiquity of these mechanisms across industries warrants their mitigation, which can be achieved by inserting technologies that reduce the likelihood that those minimum requirements will be met. Applicable technologies for newer construction include coatings, cladding, corrosion protection, and surface treatments, such as residual stress impingement (RSI). These proactive sustainment efforts can help to avoid unexpected costs, structural deficiencies, failures, and loss of life. As vehicles and parts age, the likelihood of significant defect formation due to damage, use, and environmental effects increases, which in turn decreases the required stress input needed to achieve crack initiation and growth [2]. Thus, the aging infrastructure that exists within many industries today increasingly requires proactive maintenance to mitigate aggressive environmentally induced damage. For these critical but aged components, RSI technologies are a primary candidate to achieve life extension.

RSI methods impart compressive residual stresses that reduce K/ΔK locally and combat crack initiation/propagation. These techniques are crucial for the preventative maintenance of new components, as well as for the sustainment of aging vehicles and parts. Residual stress impingement techniques, such as shot peening (SP), have been applied to metal surfaces for fatigue life improvement for over 60 years [3]. More recently, new advancements have been introduced, such as laser shock peening (LSP), low plasticity burnishing (LPB), and ultrasonic nanocrystal surface modification (UNSM), to name some common examples. These new methods have arisen to improve treatment consistency, residual stress penetration depth and stability, and surface finish, as well as other performance attributes. Reviews exist covering a range of RSI methods and their benefits, as well as expressing related concerns. McClung addressed residual stress stability and the impact of various residual stress impingement methods on fatigue [3]. Schultze and Lu have published thorough reviews of various RSI methods and their effects on the mechanical performance of materials [4][5]. Additionally, method-specific reviews exist on LSP due to this technique's rising significance. Montross reviewed the fatigue improvements achieved through LSP treatment [6], and Sundar recently reviewed the development and modern applications of LSP [7]. Sano reviewed 25 years of LSP development efforts, with a specific focus on steel applications in the nuclear power industry [8]. Priyadarsini reviewed the most common burnishing-related RSI methods (ball, roller, and LPB), and compared them against one another in residual stress penetration and stability, as well as the ability to improve fatigue, corrosion fatigue, fretting, and environmental cracking [9]. These reviews and others provide considerable insight

into the many RSI methods and common applications. However, interest has steadily increased in applying RSI methods to address environmental cracking concerns, such as surface corrosion and related defect formation, corrosion fatigue, and EAC. No review currently exists that evaluates and compares the leading RSI methods and their ability to mitigate corrosion, corrosion fatigue, and EAC susceptibility, which the present review will address.

2. Introduction to Residual Stress Impingement Methods

In general, RSI methods aim to impart compressive residual stresses into a metal surface that will offset external applied, or existing residual, tensile stresses. By reducing these stresses, the crack initiation and/or propagation rate may be decreased due to reduced stress intensity being present at the site of a small defect, or at a crack tip. These compressive residual stresses have a maximum effect while the defect remains within the compressively stressed material layer, and so the effective penetration depth achieved by a given RSI method is key. The most commonly utilized RSI treatments all have advantages as well as drawbacks that affect the final state of the alloy surface microstructure, the magnitude and depth of the imparted compressive stress, the resultant surface finish, and the efficiency of its application. Selected treatment methods will be briefly summarized.

Shot peening is one of the oldest RSI methods that are still commonly utilized today and consists of firing high-hardness shot (often glass, metal, or ceramic, depending on the target and goal) at a metal surface to impart compressive residual stress (CRS). This process is demonstrated schematically in **Figure 1**A. The SP process is controlled by the Almen intensity and coverage, where the Almen intensity reflects the effect of spot size, shot hardness, speed, flow rate, and impact angle [10]. An advantage of SP is its relative ease of application compared to some other methods, and the deep knowledge base associated with the history of its use [11]. One downside of the method is that, due to the aggressive bombardment of a surface with shot, the process parameters must be carefully controlled to achieve the desired surface roughness and consistent surface coverage, which is not as uniform as with other methods [12]. The overtreatment of a surface during SP may result in brittle cracking in the deformed surface layer, folds that may conceal defects, and even embedded shot, all of which could aggravate corrosion or crack formation [13]. The impact of shot on the alloy surface leaves dimples that form a gradient of compressive residual stress that commonly reaches 0.25–0.50 mm in depth [14][15]. The ultrasonic nanocrystal surface modification (UNSM) process uses a tungsten carbide-tipped applicator that is pressed down onto the alloy surface with a specific load and vertically vibrates at an ultrasonic frequency while moving systematically around the alloy surface [16]. The UNSM process is schematically illustrated in **Figure 1**B. This treatment is computer-directed; therefore, a uniform surface coverage is achieved that results in a low hardness increase and a low surface roughness increase in a variety of alloys [16]. UNSM commonly forms a nanocrystalline grain structure below the alloy surface, and the CRS depth tends to be similar to that seen with SP [16].

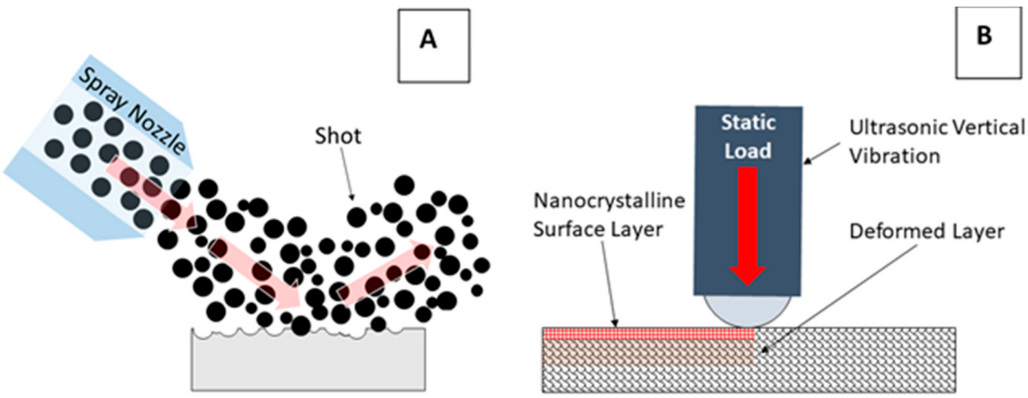

Figure 1. Schematic representations of (**A**) the shot peening process, and (**B**) the ultrasonic nanocrystal surface modification process.

Laser shock peening utilizes laser energy bombardment to impact a surface water layer and create plasma pulses through an underlying material, which drives in the CRS [6][15]. The LSP process is schematically illustrated in **Figure 2**A. The advantages of LSP include the fact that this process is computer-controlled, and each laser shot is measured and the output energy is recorded, making the process highly traceable and repeatable. The surface coverage is uniform and the CRS depths are consistent. CRS depths typically range from 0.75–1.25 mm when no ablative layer is used (**Figure 3**) [8]. When an ablative layer is used, the maximum residual stress is similar to that which is achieved without an ablative layer but the maximum penetration depth is reduced; thus, this treatment method is less common [17]. The LSP process is tuned through the laser spot size and power density applied to the alloy surface, as well as the beam overlap, all of which impact the CRS depth and final surface roughness [6][7]. One disadvantage of LSP is that this method must be utilized in

controlled settings, and strict control of the surrounding area is required due to the hazard of the laser, which can make LSP one of the more expensive RSI methods to deploy. Overtreatment through LSP occurs through the application of excessive power density, which can actually form tensile stress in the surface layer and can cause melting [18][19]. However, this is easily avoidable through preliminary research on best practices for treating a given alloy type. Lastly, LPB utilizes a hydraulically pressed bearing to apply force to an alloy surface without applying heat or causing significant microstructural deformation (**Figure 2**B) [20].

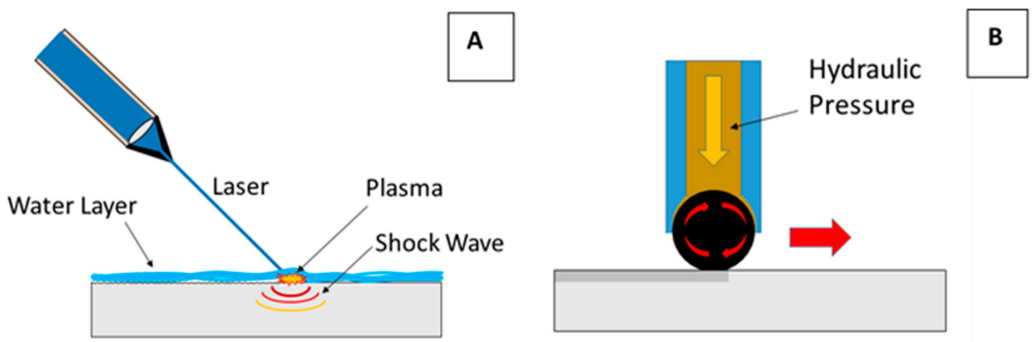

Figure 2. Schematic representations of (**A**) the laser shock peening treatment process (shown without the damping layer), and (**B**) the low plasticity burnishing process.

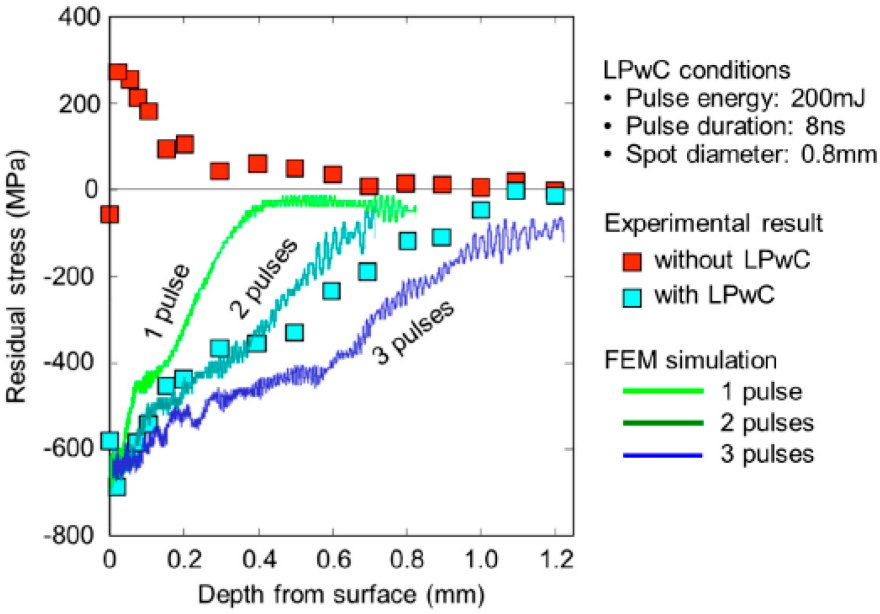

Figure 3. Impact of LSP applied 1–3 times on 316L steel weldments, compared to the residual stress profile without treatment. LPwC—laser peening without ablative coating [8]. Reprinted with permission from [8]. Copyright 2020, Metals Journal in MDPI.

This process induces minimal changes to the alloy surface profile and is proven to impart similarly high magnitude compressive residual stresses as are achieved with LSP, to a depth of roughly 1 mm or greater. An example dataset from Inconel 718 is illustrated in **Figure 4**, which compares the CRS depth and magnitude achieved by SP, LSP, and LPB [4][21].

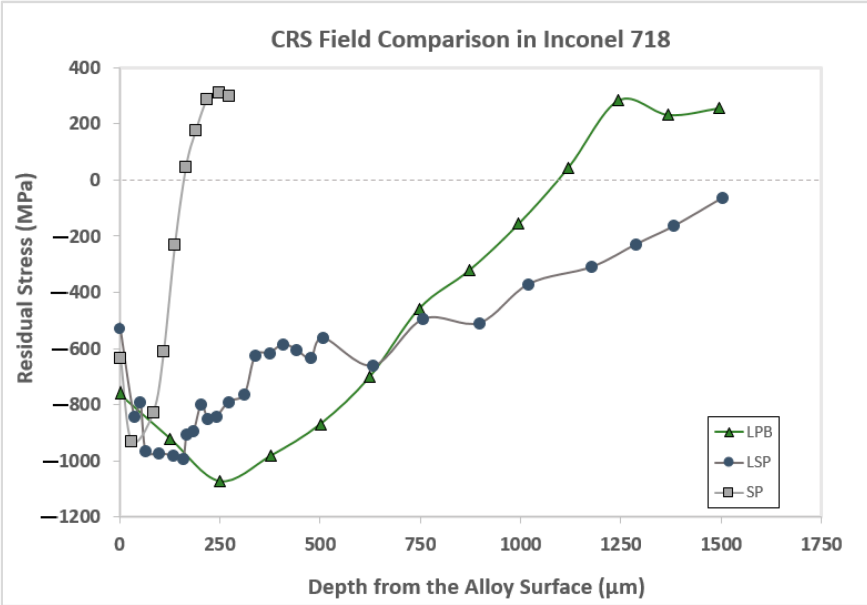

Figure 4. A comparison between the residual stress profiles achieved by SP, LSP, and LPB in Inconel 718 [21]. Reproduced with permission from [21]. Copyright 2003, Journal of Engineering for Gas Turbines and Power on behalf of ASME.

Due to the use of a hydraulically loaded ball bearing, this process is best used on open surfaces, where it can easily be utilized in a CNC machine to complement a typical machining process before the part is completed. The benefits and risks of the SP, UNSM, LSP, and LPB processes have varying impacts on the ability to improve corrosion performance in alloys of varying hardness, which will be discussed in the following section.

3. Corrosion Minimization

Corrosion is a highly surface-sensitive phenomenon; the effect of surface roughness on corrosion susceptibility is well documented in the literature [22][23]. Residual stress impingement imparts compressive stress into the alloy surface, which can improve corrosion resistance through a combination of work-hardening and grain refinement. However, RSI treatments can also increase the surface topography, which may reduce the benefit of the compressive stress and refined microstructure. Previous works have demonstrated that there is a relationship between the target alloy's passivation mechanism, the surface topography caused by the RSI, and the alloy corrosion resistance [4][24][25].

This relationship is evident when viewed across the hardness spectrum. Considering the effects of SP, firstly on low-hardness alloys, Curtis et al. evaluated shot-peened 2024-T351 (137 HV) via potentiodynamic analysis in 3.5 wt % NaCl and measured a 5-fold increase in the corrosion current density (i_{corr}) compared to the as-polished sample [26]. After 24 h in this solution at an open circuit, the 2024–T351 experienced an increased pitting rate after SP [26]. Similarly, the SP treatment of 7075-T651 (175 HV) increased the alloy's surface roughness from 0.32 µm to 5.81 µm, after which Zupanc and Grum measured a 2.5-factor increase in i_{corr} in 0.1 M NaCl [27]. When evaluating AISI 430 steel (162 HV) after SP, Peltz et al. observed a 10-fold increase in i_{corr} in 0.05 M NaCl, due mainly to the increase in surface roughness from 0.02 µm to 3.18 µm [28]. These examples demonstrate that the RSI-induced roughness in low hardness alloys detrimentally affects the passivity and corrosion resistance.

In the medium-hardness AISI 304 stainless steel (240 HV), Iswanto et al. demonstrated, in intravenous Otsu-Ringer lactate solution, that the pitting rate initially increased by as much as 20 times when SP was conducted for 5 min but decreased as SP was conducted for longer periods of time to achieve better coverage and more plastic deformation across the alloy surface [29]. Treating the 304 SS for 40 min more than doubled the surface hardness to reach 496 HV, and the pitting rate decreased from the as-polished rate of 0.042 mpy to 0.036 mpy [29]. In 316L stainless steel (220 HV), Peyre demonstrated via potentiodynamic analysis that both SP and LSP (8 GW/cm^2) achieved similar improvements in the alloy's pitting resistance, and both improved the i_{corr} in 0.5 M NaCl, despite slightly rougher surface finish as well as martensite formation following SP [30]. Interestingly, the open-circuit potential of the SP-treated 316L was also roughly 100 mV greater than the LSP-treated 316L [30]. Various authors have attributed the LSP-induced improvement in corrosion resistance to slight melting and resegregation at the alloy surface, such that the high-energy, work-hardened material is less exposed to aggravate corrosion reactions [18][31]. Considering high hardness alloys, Cuifini et al. demonstrated in 300–325 HV super duplex stainless steel that SP treatment resulted in a 3- to 4-fold increase in mass loss through salt fog

cabinet exposure [32]. Overall, these findings support the need to understand the alloy's passivity and the dependence on surface morphology before applying RSI, especially when considering techniques such as SP that can cause significant roughness and plastic deformation.

UNSM, despite achieving a more uniform surface finish than SP, can also increase corrosion susceptibility due to the added dislocation density, except in specific circumstances. In the low-hardness AZ31B (60 HV), Hou et al. demonstrated in simulated body fluid (SBF) and 0.1 M NaCl that a 2-fold increase in i_{corr} occurs following UNSM [33]. With Alloy 600 (180 HV), however, UNSM treatment below the critical amplitude was demonstrated by Kim and Kim in 1 wt % NaCl to improve the alloy passivation by creating a reactive nanocrystalline surface with low roughness, which also reduced the pitting susceptibility [34]. However, higher-amplitude treatments increased the surface roughness and created crevice-forming features that promoted aggressive chemistry formation, oxide rupture, and pitting [34]. On 4140 steel, in the annealed (183 HV) and nitrided conditions (450 HV), UNSM treatment decreased the corrosion resistance of the steel in alkaline, neutral, and acidic 3.5 wt % NaCl solutions [35]. In contrast, when Li et al. evaluated UNSM on 304SS (240 HV) in 3.5 wt % NaCl, the data revealed increased nobility and passivity, as well as improved pitting resistance [36]. Closer inspection via transmission electron microscopy (TEM) and surface analysis showed that the UNSM treatment created a cleaner surface with fewer MnS inclusions, and the nanocrystalline surface layer showed better Cr distribution, such that the passive film achieved greater Cr enrichment and improved stability [36]. It is worth noting that Kim evaluated UNSM on 316L (220 HV) in 3.5 wt % NaCl, however, and demonstrated that the improvement in pitting following UNSM depends on the level of sensitization present in the alloy; when sufficiently sensitized, UNSM can actually accelerate the pitting attack [37]. This comparison between 4140, 304SS, and 316SS demonstrates that a strong passivation mechanism in the underlying alloy may assist the RSI to improve corrosion resistance; however, the underlying alloy metallurgy, such as a highly sensitized state, can reverse this trend. In relatively high-hardness Ti-6Al-4V (380 HV), Cao et al. observed increased pitting susceptibility and a 2-fold increase in i_{corr} in SBF after applying UNSM treatment [38]. The disparities between alloys and variable RSI-related corrosion improvement demonstrate the need for a more microstructural-based understanding of why improvements are achieved in some alloys, but not in all.

LSP has a more consistent track record of improving corrosion resistance when not overly applied. In the low hardness 5083–H112 (72 HV), Yang demonstrated that LSP achieved the greatest improvement in the surface corrosion resistance when lower power density was applied for a smoother surface finish, estimating that repassivation in 3.5 wt % NaCl was more stable with less topography [39]. In 6082–T651 (85 HV), LSP evaluations across the power density range of 5.7–15.8 GW/cm^2 demonstrated that this alloy is less sensitive to power density than 5083 in dilute NaCl, since nearly all LSP treatments within the study achieved a similar reduction in pitting susceptibility, despite a 5-fold increase in surface roughness (0.72 µm to 3.74 µm in the L-direction) [19]. Trdan and Grum later demonstrated that LSP improves the polarization resistance of 6082–T651 by 25-fold, expands the passive electrode voltage region on the potentiodynamic curve, and decreases i_{corr} as much as 10-fold compared to untreated 6082–T651 in 0.6 M NaCl [18]. In 7075–T6 (175 HV), Aravamudhan demonstrated, through potentiodynamic polarization, that LSP reduced i_{corr} by 2–3 times in 3.5 wt % NaCl [40]. Pitting was observed to occur preferentially near the valleys formed during LSP treatment on the 7075–T6, where chemistry could more easily acidify, and the magnitude of valley formation depended on the power density selection [40]. Considering LPB, Cao demonstrated that LPB reduced mass loss in AZ31B (60 HV) in 5 wt % NaCl over 7 days' immersion, and the corrosion rate was more consistent than that measured on the non-treated samples [41]. The main cause for this improvement was hypothesized to be the smaller grain size and reduction of intermetallic phases near the alloy surface, as well as the smooth surface finish and aligned crystalline orientation generally caused by the LPB, all of which promote corrosion resistance in Mg (but this is likely different in other alloys, especially regarding the effect of grain size) [41]. These collective findings demonstrate that the impact of RSI methods on corrosion susceptibility is largely dependent on alloy, the intensity of surface treatment, and the resulting microstructure. The impact of microstructural changes and surface deformation on the intermetallic presence and oxide stability will also play a significant role in the final corrosion susceptibility. If properly applied, these results demonstrate that specific RSI/alloy combinations and processing could reduce a component's tendency to corrode over a service life, which is an added benefit to well-known CRS-induced fatigue life improvements.

4. Fatigue Mitigation

Prior to evaluating the effects of RSI on the rather complex corrosion fatigue phenomenon, a brief review of mechanical fatigue and known RSI impacts on fatigue is necessary. Fatigue performance depends on a variety of factors including, but not limited to, an alloy's microstructural cleanliness, machining and surface finish, environment, residual stresses, and cyclic load schedule. Deleterious residual stresses may be imparted through manufacturing processes, such as forging, casting, forming, and machining and these stresses will impact fatigue performance, often in complex ways as the

stresses redistribute and relax with time in service [3]. These manufacturing stresses, as well as the impact of the cyclic load schedule, have been addressed successfully in a wide range of alloys through the development and utilization of optimized RSI methods. These successes are typically separated by the RSI impact on fatigue initiation, and on fatigue propagation.

5. Mitigation of Environmentally Assisted Cracking

Environmentally assisted cracking is a common threat to achieving component design life in service, especially as the use of higher-strength alloys becomes increasingly common in aggressive conditions. Despite the diversity of mechanisms that exist that cause EAC, all processes require sufficient applied stress to exceed a threshold stress intensity for a given corrosive environment. When utilizing SP to evaluate hydrogen embrittlement susceptibility in PSB1080 steel (520 HV), Li et al. observed via slow strain rate testing that increasingly intense SP treatment improved the elongation achieved during testing, which is contrary to typical work-hardening behavior [42]. Hydrogen permeation evaluations demonstrated that the dislocation fields induced by the SP reduced hydrogen diffusion into the steel by acting as a hydrogen trap, and the dislocation density increased with the SP intensity [42]. The HE-related crack growth became increasingly branched in the SP test specimens as well. In static bend testing, Brown et al. demonstrated through seacoast exposure that 2014-T651 (155 HV) and 7079-T651 (150 HV) both benefitted from SP treatment, where the residual stress mitigated the onset of SCC failure by 3 months in 2014 and 4+ years in 7079 [43]. In more aggressive alternate immersion settings, by contrast, the SP had a negligible effect in 2014-T651, and extended the alloy life by 4 months in the 7079-T651 [43]. The authors' conclusion from these results was that the characteristically faster pitting rates in 2024-T651 quickly penetrated through the 0.25–0.50 mm compressive surface layer, which greatly decreased the efficacy of the SP in more corrosive conditions [43]. The 7079-T651, by contrast, experienced slower pitting, so that the effect of the SP treatment lasted much longer. These authors also observed that the SP treatment distorted and bent the grain boundaries in the compressive surface layer, which created a more tortuous crack path that slowed crack initiation and the early stages of crack advances [43].

Numerous successful applications of LSP and LPB for EAC mitigation have been published for 316L (220 HV) and 304L (240 HV), for nuclear applications in cooling water environments, such as that shown in **Figure 5** [44]. Scheel et al. demonstrated in boiling $MgCl_2$ that the LPB treatment halted EAC in 304L heat-affected zones [45]. Sundar et al. performed similar testing on sensitized 304L and observed increasingly lower EAC susceptibility as the LSP power density was increased from 3.6 GW/cm^2 to 6.4 GW/cm^2 [46]. Higher power levels of LSP have also been demonstrated to reduce 304L susceptibility to intergranular corrosion by melting the surface; however, this process may also introduce deleterious tensile stresses and will not be reviewed [31][47].

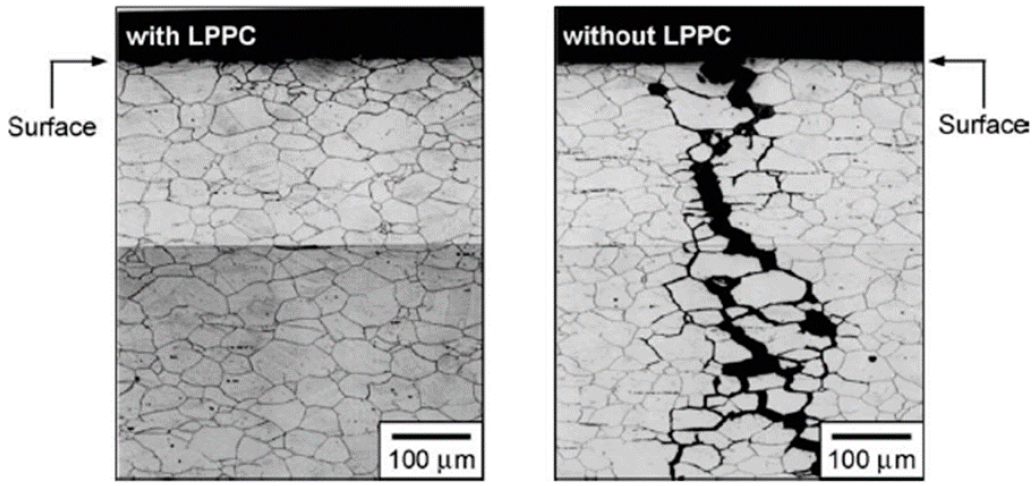

Figure 5. Successful mitigation of stress corrosion cracking in 316L in cooling water due to laser shock peening treatment without an ablative coating [44]. Reprinted with permission from [44]. Copyright 2006, Materials Science and Engineering A on behalf of Elsevier.

In AZ31B (83 HV), Zhang et al. demonstrated that LSP reduced the SCC in a NaOH environment through the added CRS and finer surface microstructure [48]. However, studies on brass alloys 260 and 280 (80 HV) demonstrated that LSP treatment mitigated EAC only when certain microstructures/compositions were present (in this case, higher Zn content in brass 280), such that the dezincification was reduced by the added CRS and dislocation densities [49].

Regarding UNSM, Telang et al. utilized this treatment, combined with annealing, to promote special grain boundary junctions in Alloy 600, which reduced the sensitization of the surface and reduced EAC susceptibility in tetrathionate

solution [50]. In multi-layered steel, Jo et al. evaluated UNSM treatment for its effect on hydrogen permeability and determined that the 0.2 mm-deep CRS zone created by UNSM acted as a strong hydrogen barrier by storing compressive residual stress, as well as by trapping the hydrogen in the high dislocation densities, twin boundaries, and grain boundaries [51]. These results are in agreement with the SP results from Li et al. [42], demonstrating a consistent capability to reduce hydrogen permeability via RSI treatment to mitigate EAC in the CRS layer. Additionally, Takakuwa et al. demonstrated via modeling that CRS will also reduce hydrogen concentration at an environmental crack tip, by lowering the hydrostatic stress [52]. Altogether, these findings demonstrate that the main means through which RSI treatment may impact EAC susceptibility is:

- Increased resistance to hydrogen permeability from the treated surface through hydrogen trapping in the CRS zone;
- Reduced surface corrosion to delay corrosion-related defect formation, stress concentration, and exceeding of the threshold K (K_{TH}); and
- Reduction of the hydrostatic stress at the crack tip by reducing the resolved tensile stress, which reduces the driving force for hydrogen diffusion into the fracture process zone.

This technical understanding of the effects of RSI on corrosion, corrosion fatigue, and EAC provides substantive background to understand the case studies of successful RSI applications in various industries. Additionally, applied research efforts will be reviewed with an emphasis on potential new uses of RSI technology.

References

1. Anderson, T.L. Fracture Mechanics: Fundamentals and Applications, 4th ed.; CRC Press: Boca Raton, FL, USA, 2017; pp. 471–578.
2. Shih, C.F.; DeLorenzi, H.G.; Andrews, W.R. Studies on crack initiation and stable crack growth. In Elastic-Plastic Fractu re; ASTM International: West Conshohocken, PA, USA, 2009; pp. 65–120.
3. Mcclung, R.C. A literature survey on the stability and significance of residual stresses during fatigue. Fatigue Fract. En g. Mater. Struct. 2007, 30, 173–205.
4. Schulze, V. Modern Mechanical Surface Treatment: States, Stability, Effects; Wiley-VCH: Weinheim, Germany, 2005; p p. 60–350.
5. Lu, J. (Ed.) Handbook on Residual Stress, 2nd ed.; Society for Experimental Mechanics: Bethel, CT, USA, 2005; pp. 30 –50.
6. Montross, C.S. Laser shock processing and its effects on microstructure and properties of metal alloys: A review. Int. J. Fatigue 2002, 24, 1021–1036.
7. Sundar, R.; Ganesh, P.; Gupta, R.K.; Ragvendra, G.; Pant, B.K.; Kain, V.; Ranganathan, K.; Kaul, R.; Bindra, K.S. Lase r Shock Peening and its Applications: A Review. Lasers Manuf. Mater. Process. 2019, 6, 424–463.
8. Sano, Y. Quarter Century Development of Laser Peening without Coating. Metals 2020, 10, 152–163.
9. Priyadarsini, C.; Ramana, V.V.; Prabha, K.A.; Swetha, S. A Review on Ball, Roller, Low Plasticity Burnishing Process. M ater. Today Proc. 2019, 18, 5087–5099.
10. Maamoun, A.H.; Elbestawi, M.A.; Veldhuis, S.C. Influence of Shot Peening on AlSi10Mg Parts Fabricated by Additive M anufacturing. J. Manuf. Mater. Process. 2018, 2, 40.
11. Al-Obaid, Y.F. A Rudimentary Analysis of Improving Fatigue Life of Metals by Shot-Peening. J. Appl. Mech. 1990, 57, 30 7–312.
12. Maleki, E.; Unal, O.; Guagliano, M.; Bagherifard, S. The effects of shot peening, laser shock peening and ultrasonic na nocrystal surface modification on the fatigue strength of Inconel 718. Mater. Sci. Eng. A 2021, 810, 141029–141040.
13. Zhuang, W.; Liu, Q.; Djugum, R.; Sharp, P.; Paradowska, A. Deep surface rolling for fatigue life enhancement of laser cl ad aircraft aluminium alloy. Appl. Surf. Sci. 2014, 320, 558–562.
14. Ferreira, N.; Antunes, P.V.; Ferreira, J.A.M.; Costa, J.; Capela, C. Effects of Shot-Peening and Stress Ratio on the Fatig ue Crack Propagation of AL 7475-T7351 Specimens. Appl. Sci. 2018, 8, 375.
15. Gujba, A.K.; Medraj, M. Laser Peening Process and Its Impact on Materials Properties in Comparison with Shot Peenin g and Ultrasonic Impact Peening. Materials 2014, 7, 7925–7974.

16. Amanov, A.; Pyun, Y. A comprehensive review of nanostructured materials by ultrasonic nanocrystal surface modificatio n technique. J. Eng. 2015, 2015, 144–149.

17. González, J.A.P.; Gomez-Rosas, G.; Ocaña, J.L.; Molpeceres, C.; Banderas, A.; Porro, J.; Morales, M. Effect of an abs orbent overlay on the residual stress field induced by laser shock processing on aluminum samples. Appl. Surf. Sci. 20 06, 252, 6201–6205.

18. Trdan, U.; Grum, J. Investigation of Corrosion Behaviour of Aluminium Alloy Subjected to Laser Shock Peening without a Protective Coating. Adv. Mater. Sci. Eng. 2015, 2015, 705306.

19. Trdan, U.; Grum, J. Evaluation of corrosion resistance of AA6082-T651 aluminium alloy after laser shock peening by m eans of cyclic polarisation and ElS methods. Corros. Sci. 2012, 59, 324–333.

20. Sticchi, M.; Schnubel, D.; Kashaev, N.; Huber, N. Review of Residual Stress Modification Techniques for Extending the Fatigue Life of Metallic Aircraft Components. Appl. Mech. Rev. 2014, 67, 010801.

21. Zhuang, W.; Wicks, B. Mechanical Surface Treatment Technologies for Gas Turbine Engine Components. J. Eng. Gas. Turbines Power 2003, 125, 1021–1025.

22. Evgeny, B.; Hughes, T.; Eskin, D. Effect of surface roughness on corrosion behaviour of low carbon steel in inhibited 4 M hydrochloric acid under laminar and turbulent flow conditions. Corros. Sci. 2016, 103, 196–205.

23. Sohrabi, M.J.; Mirzadeh, H.; Dehghanian, C. Unraveling the effects of surface preparation on the pitting corrosion resist ance of austenitic stainless steel. Arch. Civ. Mech. Eng. 2020, 20, 8.

24. Trung, P.Q.; Khun, N.W.; Butler, D.L. Effect of Shot Peening Process on the Fatigue Life of Shot Peened Low Alloy Ste el. J. Eng. Mater. Technol. 2017, 140, 011013.

25. Reggiani, B. Experimental Investigation on the Effect of Shot Peening and Deep Rolling on the Fatigue Response of Hi gh Strength Fasteners. Metals 2019, 9, 1093.

26. Curtis, S.A.; Rios, E.R.D.L.; Rodopoulos, C.A.; Romero, J.S.; Levers, A. Investigating the Benefits of Controlled Shot P eening on Corrosion Fatigue of Aluminium Alloy 2024 T351. In Shot Peening; Wagner, L., Ed.; Wiley-VCH Verlag Gmb H & Co. KGaA: Weinheim, Germany, 2003; pp. 264–270.

27. Zupanc, U.; Grum, J. Effect of pitting corrosion on fatigue performance of shot-peened aluminium alloy 7075-T651. J. Mater. Process. Technol. 2010, 210, 1197–1202.

28. Peltz, J.D.S.; Beltrami, L.V.R.; Kunst, S.R.; Brandolt, C.; Malfatti, C.D.F. Effect of the Shot Peening Process on the Corr osion and Oxidation Resistance of AISI430 Stainless Steel. Mater. Res. 2015, 18, 538–545.

29. Iswanto, P.T.; Malau, V.; Priyambodo, B.H.; Wibowo, T.N.; Amin, N. Effect of Shot-Peening on Hardness and Pitting Cor rosion Rate on Load-Bearing Implant Material AISI 304. Mater. Sci. Forum 2017, 901, 91–96.

30. Peyre, P.; Scherpereel, X.; Berthe, L.; Carboni, C.; Fabbro, R.; Béranger, G.; Lemaitre, C. Surface modifications induce d in 316L steel by laser peening and shot-peening. Influence on pitting corrosion resistance. Mater. Sci. Eng. A 2000, 2 80, 294–302.

31. Yue, T.M.; Yan, L.; Chan, C. Stress corrosion cracking behavior of Nd:YAG laser-treated aluminum alloy 7075. Appl. Su rf. Sci. 2006, 252, 5026–5034.

32. Ciuffini, A.F.; Barella, S.; Martínez, L.B.P.; Mapelli, C.; Pariente, I.F. Influence of Microstructure and Shot Peening Treat ment on Corrosion Resistance of AISI F55-UNS S32760 Super Duplex Stainless Steel. Materials 2018, 11, 1038.

33. Hou, X.; Qin, H.; Gao, H.; Mankoci, S.; Zhang, R.; Zhou, X.; Ren, Z.; Doll, G.L.; Martini, A.; Sahai, N.; et al. A systemati c study of mechanical properties, corrosion behavior and biocompatibility of AZ31B Mg alloy after ultrasonic nanocrysta l surface modification. Mater. Sci. Eng. C 2017, 78, 1061–1071.

34. Kim, K.T.; Kim, Y.S. Effect of the Amplitude in Ultrasonic Nano-crystalline Surface Modification on the Corrosion Propert ies of Alloy 600. Corr. Sci. Tech. 2019, 18, 196–205.

35. Ren, Z.; Hou, X.; Dong, Y.; Ye, C. Effect of Nanocrystallization-Assisted Nitriding on the Corrosion Behavior of AISI 414 0 Steel. In Proceedings of the ASME 2016 11th International Manufacturing Science and Engineering Conference, Blac ksburg, VA, USA, 27 June 27–1 July 2016; 2016; Volume 49903, p. V002T01A008.

36. Li, S.; Ren, Z.; Dong, Y.; Ye, C.; Cheng, G.; Cong, H. Enhanced Pitting Corrosion Resistance of 304 SS in 3.5 wt% Na Cl by Ultrasonic Nanocrystal Surface Modification. J. Electrochem. Soc. 2017, 164, C682–C689.

37. Kim, K.-T.; Lee, J.-H.; Kim, Y.-S. Effect of Ultrasonic Nano-Crystal Surface Modification (UNSM) on the Passivation Beh avior of Aged 316L Stainless Steel. Materials 2017, 10, 713.

38. Cao, X.; Xu, X.; Wang, C.; Pyoun, Y.; Wang, Q. Effect of Ultrasonic Surface Impact on the Fatigue Behavior of Ti-6Al-4 V Subject to Simulated Body Fluid. Metals 2017, 7, 440.

39. Yang, Y.; Zhou, W.; Tong, Z.; Chen, L.; Yang, X.; Larson, E.A.; Ren, X. Electrochemical Corrosion Behavior of 5083 Aluminum Alloy Subjected to Laser Shock Peening. J. Mater. Eng. Perform. 2019, 28, 6081–6091.
40. Aravamudhan, B.H. Study of the Effect of Laser Shock Peening on Corrosion Behavior of Aluminum Alloy 7075. Master's Thesis, Department Mechanical and Materials Engineering, University of Cincinatti, Cincinatti, OH, USA, July 2018.
41. Cao, C.; Zhu, J.; Tanaka, T.; Pham, D.N. Investigation of Corrosion Resistance Enhancement for Biodegradable Magnesium Alloy by Ball Burnishing Process. Int. J. Autom. Technol. 2020, 14, 175–183.
42. Li, X.; Zhang, J.; Wang, Y.; Ma, M.; Shen, S.; Song, X. The dual role of shot peening in hydrogen-assisted cracking of PSB1080 high strength steel. Mater. Des. 2016, 110, 602–615.
43. Brown, B.F. Stress Corrosion Cracking in High Strength Steels and in Titanium and Aluminum Alloys; Naval Research Laboratory: Washington, DC, USA, 1972; p. A030873.
44. Sano, Y.; Obata, M.; Kubo, T.; Mukai, N.; Yoda, M.; Masaki, K.; Ochi, Y. Retardation of crack initiation and growth in austenitic stainless steels by laser peening without protective coating. Mater. Sci. Eng. A 2006, 417, 334–340.
45. Scheel, J.E.; Hornbach, D.J.; Prevey, P.S. Mitigation of stress corrosion cracking in nuclear weldments using low plasticity burnishing. In Proceedings of the 16th International Conference on Nuclear Engineering, Orlando, FL, USA, 11–15 May 2008.
46. Sundar, R.; Ganesh, P.; Kumar, B.S.; Gupta, R.K.; Nagpure, D.C.; Kaul, R.; Ranganathan, K.; Bindra, K.S.; Kain, V.; Oak, S.M.; et al. Mitigation of Stress Corrosion Cracking Susceptibility of Machined 304L Stainless Steel Through Laser Peening. J. Mater. Eng. Perform. 2016, 25, 3710–3724.
47. Gupta, R.K.; Sundar, R.; Kumar, B.S.; Ganesh, P.; Kaul, R.; Ranganathan, K.; Bindra, K.S.; Kain, V.; Oak, S.M.; Kukreja, L.M. A Hybrid Laser Surface Treatment for Refurbishment of Stress Corrosion Cracking Damaged 304L Stainless Steel. J. Mater. Eng. Perform. 2015, 24, 2569–2576.
48. Zhang, L.-J.; Zhang, H.-B.; Lei, X.-W.; Wang, R.; Han, B.-F.; Zhang, J.-X.; Na, S.-J. Laser processing of Mg-10Li-3Al-3Zn alloy: Part II- Improving corrosion resistance of multi-phase Mg alloys by laser surface processing. J. Manuf. Process. 2020, 56, 571–580.
49. Lisenko, N.; Evans, C.D.; Yao, Y.L. Effect of brass composition and phases on stress corrosion mitigation by laser shock peening. Manuf. Lett. 2019, 23, 5–8.
50. Telang, A.; Gill, A.S.; Tammana, D.; Wen, X.; Kumar, M.; Teysseyre, S.; Mannava, S.R.; Qian, D.; Vasudevan, V.K. Surface grain boundary engineering of Alloy 600 for improved resistance to stress corrosion cracking. Mater. Sci. Eng. A 2015, 648, 280–288.
51. Jo, M.C.; Yoo, J.; Amanov, A.; Song, T.; Kim, S.-H.; Sohn, S.S.; Lee, S. Ultrasonic nanocrystal surface modification for strength improvement and suppression of hydrogen permeation in multi-layered steel. J. Alloys Compd. 2021, 885, 160975–160985.
52. Takakuwa, O.; Nishikawa, M.; Soyama, H. Numerical simulation of the effects of residual stress on the concentration of hydrogen around a crack tip. Surf. Coat. Technol. 2012, 206, 2892–2898.